Computer Assisted Mechanics and Engineering Sciences, 7: 743–755, 2000.

On the boundary crises of chaotic attractors in nonlinear oscillators

Elżbieta Tyrkiel, Wanda Szemplińska-Stupnicka and Andrzej Zubrzycki
Institute of Fundamental Technological Research, Polish Academy of Sciences, ul. Świętokrzyska 21, 00-049 Warszawa, Poland

(Received November 3, 1999)

In nonlinear dissipative mechanical systems, bifurcations of chaotic attractors called *boundary crises* appear to be the cause of most sudden changes in chaotic dynamics. They result in a sudden loss of stability of chaotic attractor, together with destruction of its basin of attraction and its disappearance from the phase portrait. Chaotic attractor is destroyed in the collision with an unstable orbit (*destroyer saddle*) sitting on its basin boundary, and the structure of the saddle defines the type of the crisis – *regular* or *chaotic* one. In the paper we exemplify both types of the boundary crisis by using a mathematical model of the symmetric twin-well Duffing oscillator; we consider the regular boundary crisis of the cross-well chaotic attractor, and the chaotic boundary crisis of the single-well chaotic attractor. Our numerical analysis makes use of the underlying topological structure of the phase space, namely the geometry of relevant invariant manifolds, as well as the structure of basins of attraction of the coexisting attractors. The study allows us to establish some relevant relations between the properties of the regular and chaotic boundary crisis, and to outline the differences that result mainly in the post-crisis system behavior.

1. Introduction

Nonlinear phenomena in mechanical systems play an important role in engineering dynamics, because their appearance may disturb a desired motion of an engineering device, or even may produce irregular and dangerous oscillations. In the study of a behavior of dissipative nonlinear oscillators, particular attention should be paid to *crises*, i.e. the bifurcations which are catastrophic, in the sense, that the current path of a stable solution (attractor) undergoes a discontinuous change (annihilation, destruction, strict loss of stability). This results in a transient trajectory making a "jump" in a phase space to a disconnected coexisting attractor. If more than one other attractor is available, the final outcome may depend very sensitively on how the catastrophe is realized, and in this sense may be indeterminate.

While steady-state chaotic motion (*chaotic attractor*) of a system is generally less desirable than a regular, periodic motion, it has at least the virtue of being statistically stationary and confined to a well-defined region of phase-space. The situation near the crisis is drastically worse, because the time-history of a system trajectory may be completely different in time intervals of arbitrary duration.

Bifurcations of chaotic attractors called *boundary crises* result in a sudden loss of stability of the chaotic attractor together with destruction of its basin of attraction and its disappearance from the phase portrait. The key event underlying the phenomenon is a collision of the chaotic attractor with an unstable periodic orbit (a saddle) not on the attractor, which takes place in the phase space as the system parameter p passes through some critical value p_c. For this particular unstable orbit, the term *destroyer saddle* is used. Such collisions were widely reported in recent publications, e.g. [2, 5, 7, 8, 13].

The structure of the invariant manifolds of the destroyer saddle governs many aspects of the crisis.

If the outset (unstable manifold) of the saddle which branches away from the chaotic attractor is not tangled prior to the crisis, we deal with the case of *regular boundary crisis*, and the saddle is called *regular destroyer saddle*. The outset tends to the attractor, which coexists with the chaotic one, while the other outset tends to the chaotic attractor and forms the closure of it. In contrast, if the outset of the destroyer saddle which branches away from the chaotic attractor is tangled (i.e. it is after the homoclinic bifurcation) prior to the crisis, we face the phenomenon of *chaotic boundary crisis*, and the saddle is called *chaotic destroyer saddle*. In the latter case, one of the outsets of the destroyer saddle still tends to the chaotic attractor, while the other, tangled outset does not tend to any coexisting attractor, but involves a non-attracting chaotic set with an infinite number of unstable orbits and a highly complicated, horseshoe-type dynamics [5].

The collision of the destroyer saddle with the chaotic attractor implies a homoclinic bifurcation of the saddle [7]. Thus the critical parameter p_c of the boundary crisis can be determined by computation of a tangency condition of invariant manifolds of the unstable orbit. The aim of our paper is to outline also the other characteristic properties of the system which accompany either regular or chaotic boundary crisis, such as: geometrical equivalence of the invariant manifolds which account for the crisis, period of the destroyer saddle, structure of the boundaries of basins of attraction, post-crisis chaotic transients and predictability of the final outcome. We exemplify both types of the boundary crisis phenomena by using a dissipative, symmetric twin-well potential Duffing system. For more information and details see [9–12].

It is necessary to emphasize that the geometrical and qualitative properties of chaotic dynamics of strongly nonlinear systems cannot be analyzed by approximate analytical methods; the analysis necessitates numerical computations which are mainly based on numerical integration of system trajectories. Hence, we are confined to draw the conclusions based on "numerical evidence" only. Numerical results presented in the paper are mainly obtained by the aid of the nonlinear software package *Dynamics* [4].

2. The symmetric twin-well Duffing oscillator and its chaotic attractors

We examine the boundary crisis phenomena that appear in a dissipative, externally driven, symmetric twin-well potential Duffing system, governed by the second order differential equation in the form

$$\ddot{u} + k\dot{u} - \alpha u + \beta u^3 = A\cos\bar{\omega}\tau, \qquad \alpha, \beta > 0, \tag{1}$$

where u stands for a displacement, dots denote differentiating with respect to time τ, k represents damping coefficient, and A, $\bar{\omega}$ denote the amplitude and frequency of the driving force, respectively. Thus, the quartic potential of the system

$$V(x) = -\frac{1}{2}\alpha u^2 + \frac{1}{4}\beta u^4$$

possesses two wells with minima: $u_{1,2} = \pm\sqrt{\frac{\alpha}{\beta}}$, separated by a smooth potential barrier (hilltop) with maximum at $u = 0$. The linear natural frequency of undamped, small oscillations around the stable equilibrium position $u_{1(2)}$ is $\Omega_0 = \sqrt{2\alpha}$.

By introducing the two changes of variables,

$$t = \tau\sqrt{2\alpha}, \qquad x = u\sqrt{\frac{\beta}{\alpha}},$$

we reduce the equation (1) to the general "standard form" [10]

$$\ddot{x} + h\dot{x} - \frac{1}{2}x + \frac{1}{2}x^3 = F\cos\omega t, \qquad T = \frac{2\pi}{\omega}, \tag{2}$$

where:

$$h = \frac{k}{\sqrt{2\alpha}}, \qquad F = \frac{A}{2\alpha}\sqrt{\frac{\beta}{\alpha}}, \qquad \omega = \frac{\bar{\omega}}{\sqrt{2\alpha}},$$

and dots denote differentiating with respect to nondimensional time t. The standard system (2) satisfies the following conditions:

- the two stable equilibrium positions are located at $x_{1,2} = \pm 1$, while the unstable equilibrium position (hilltop) corresponds to $x = 0$;
- the linear natural frequency $\Omega_0 = 1$.

In the paper, we are confined to the region of driving frequency ω in the neighborhood of the *primary nonlinear resonance*, i.e. for $\omega \approx \Omega_0 = 1$. Under weak forcing there are two stable solutions, a T-periodic orbit encircling each potential minimum. With increasing forcing, the softening effect of the restoring force causes a familiar nonlinear response with hysteresis, resulting in a second coexisting T-periodic orbit in each well. The response amplitude of this second periodic motion measured from the potential minimum is larger than that of the original one; the larger amplitude solution is called the *resonant attractor*, while the coexisting less amplitude solution is referred to as the *nonresonant attractor*. Both single-well oscillations are separated by the unstable T-periodic orbit (*single-well saddle*). The unstable solution which corresponds to the maximum of the potential energy is represented by the T-periodic unstable orbit (*hilltop saddle*).

When the forcing amplitude is large enough, the steady-state stable solution overcomes the potential barrier; the system can either jump from one well to the other in a random-like manner, or exhibit regular periodic oscillations that encircle both potential wells. The former response is referred to as the *cross-well chaotic attractor*, when the latter one – as the cross-well T-periodic attractor (*large orbit*).

Throughout our paper, we use the following notation: S'_n, S'_r (S''_n, S''_r) denote the nonresonant and resonant attractors in the left (right) well, respectively; D' (D'') are the corresponding single-well saddles, S_L is the cross-well T-periodic attractor (large orbit), D_L denotes the cross-well T-periodic saddle associated with S_L attractor, D_H stands for the hilltop saddle.

Schematic diagram of regions of existence of the various attractors in the system parameter plane F–ω, at fixed damping ($h = 0.1$ throughout this study), is displayed in Fig. 1. The lines *snB* and *snA* denote the critical thresholds of saddle-node bifurcations giving birth to resonant and nonresonant single-well attractors, respectively. Within the triangle-like domain confined by *snB*, *snA* and *PD* stability limits the system exhibits primary nonlinear resonance oscillations with hysteresis, i.e. with two T-periodic attractors in each well (the corresponding continuous-time trajectories in a phase plane x–$\dot{x}$ are shown in Fig. 2a). On increasing the forcing parameter F (or decreasing the driving frequency ω), the resonant attractors S'_r, S''_r undergo the first period doubling bifurcation (line *PD* in Fig. 1), followed by a *cascade of period-doublings*, the cascade which was found in many physical systems, and which is regarded in nonlinear dynamics as a generic route to chaos [1]. The schematic bifurcation diagram of the period-doubling cascade in the x_P–F (or x_P–ω) plane, where x_P denotes the Poincaré displacement on the Poincaré section plane, is shown in Fig. 2b. At the end of the cascade, the *single-well chaotic attractor* is observed in a narrow band of the control parameter, and this attractor is finally annihilated in a *boundary crisis* scenario, denoted by **cr1** line.

At $F < F_1$, after the boundary crisis, the single-well chaotic attractor is erased from the phase portrait, and the system renders with only nonresonant attractor $S'_n(S''_n)$ in each well (Fig. 2c). At $F > F_1$, the boundary crisis of the single-well chaos gives rise to explosive bifurcation which leads to the creation of the cross-well chaotic attractor [3, 14]. In the region of frequency between the two codimension–two bifurcation points ($\omega_1 < \omega < \omega_2$ in Fig. 1), an increase of the forcing parameter F leads to another scenario of creating the cross-well chaos: after exceeding the saddle-node bifurcation

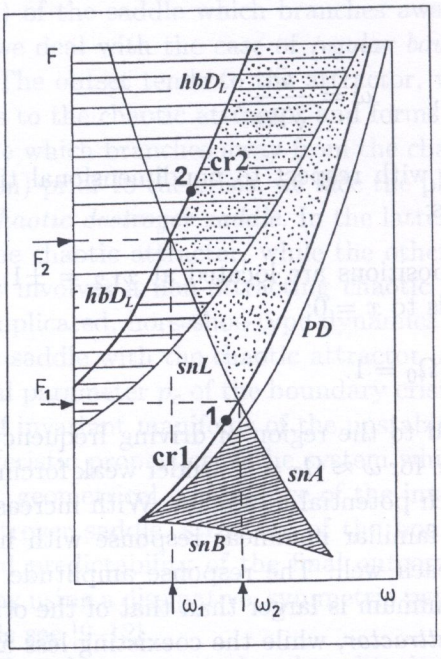

Fig. 1. Schematic diagram of regions of existence of different attractors in the twin-well potential Duffing oscillator. ▨ – coexistence of the T-periodic resonant (S'_r, S''_r) and nonresonant (S'_n, S''_n) single-well attractors (region of resonant hysteresis); ⁘ – cross-well chaotic attractor; ▤ – T-periodic cross-well resonant attractor (large orbit) S_L; *snA, snB, snL* – saddle-node bifurcations; PD – first period-doubling bifurcation of the single-well resonant attractors; hbD_L – homoclinic bifurcation of the cross-well saddle D_L; **cr1, cr2** – boundary crises of chaotic attractors

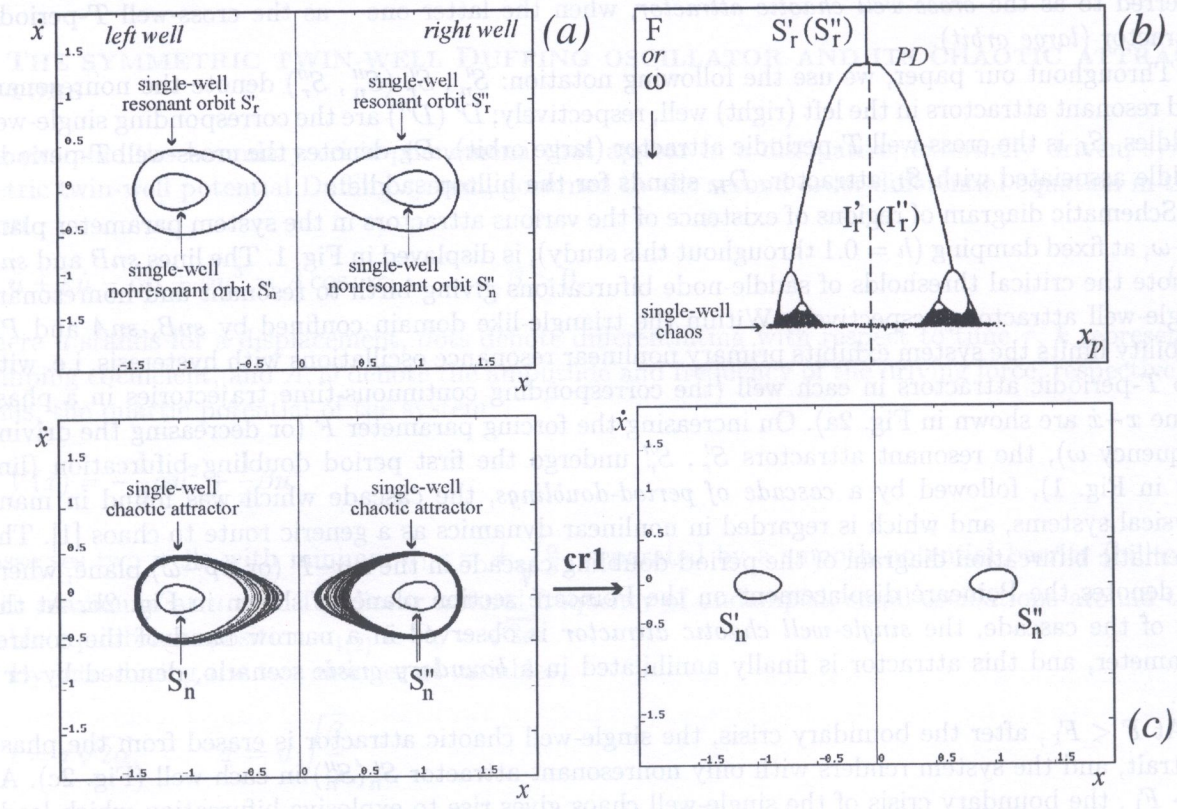

Fig. 2. (a) coexistence of resonant and nonresonant T-periodic single-well oscillations; (b) bifurcation diagram of the period-doubling cascade of the single-well resonant attractor; (c) boundary crisis of the single-well chaotic attractor, in the region of forcing values $F < F_1$

denoted by *snA* line, the two single-well attractors lose stability in favor of the cross-well chaotic attractor (we face here the phenomenon of intermittency [9]).

Within the domain confined by *snL*, *snA* and **cr1** lines (dotted region) the cross-well chaotic attractor exists as a unique attractor of the system. At the threshold value denoted by *snL* a pair of the T-periodic resonant cross-well orbits appears – the attractor S_L (large orbit) and the saddle D_L are born in the saddle-node bifurcation. Thus, within the region of control plane confined by *snL*, *snA* and **cr2** lines (dotted-dashed region), the cross-well chaotic attractor coexists with the T-periodic cross-well attractor S_L. At $F > F_2$, the cross-well chaos is annihilated by a boundary crisis, denoted by **cr2** line, after which the large orbit S_L remains the unique attractor of the system (Fig. 3).

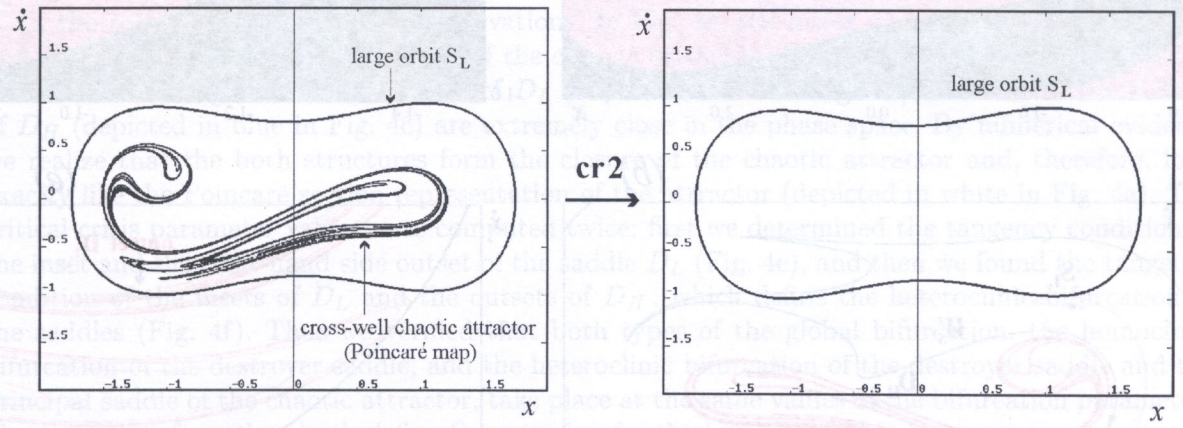

Fig. 3. Boundary crisis of the cross-well chaotic attractor, in the region of forcing values $F > F_2$; the large orbit attractor is shown as a continuous time trajectory, while the chaotic attractor – as the Poincaré section representation

Chaotic attractors are characterized by the fundamental period, i.e. the least period of an unstable orbit embedded in the attractor. The unstable orbit with the fundamental period is called the *principal saddle* of the chaotic attractor.

In Sec. 3 of this paper we first consider the boundary crisis of the cross-well chaotic attractor, which is an example of the regular boundary crisis. The phenomenon was studied in detail in [9], with an attention focused on the neighborhood of the codimension–two bifurcation point at $F = F_2$ (i.e. the point of intersection of the saddle-node bifurcation *snA*, and the homoclinic bifurcation of the cross-well saddle D_L (line hbD_L) in the control plane, Fig. 1). In Sec. 4 the boundary crisis of the single-well chaotic attractor, in the region of $F < F_1$, is discussed . The latter case was already reported by a number of researchers (e.g. [8]), and is celebrated as an example of the chaotic boundary crisis.

3. Regular boundary crisis of the cross-well chaotic attractor

In this section we consider the boundary crisis of the cross-well chaotic attractor in the region of $F > F_2$ (line **cr2**, point **2** in Fig. 1). The principal saddle of the chaotic attractor is the hilltop saddle D_H, with the fundamental period T. In the region of control plane that precedes the crisis threshold, the cross-well chaotic attractor coexists with the cross-well T-periodic attractor S_L (large orbit). At the boundary crisis denoted by **cr2** line the chaotic attractor is destroyed in the collision with the T-periodic cross-well saddle D_L.

In Fig. 4a we show (in the x–$\dot{x}$ plane) the basin-phase portrait of the two coexisting attractors, while in Fig. 4b – invariant manifolds of the T-periodic saddle D_L, prior to the boundary crisis of the cross-well chaos. It is clearly seen that the boundary of basins of attraction of the two attractors is smooth and is defined by the insets of the saddle D_L. The outset of D_L which branches away from

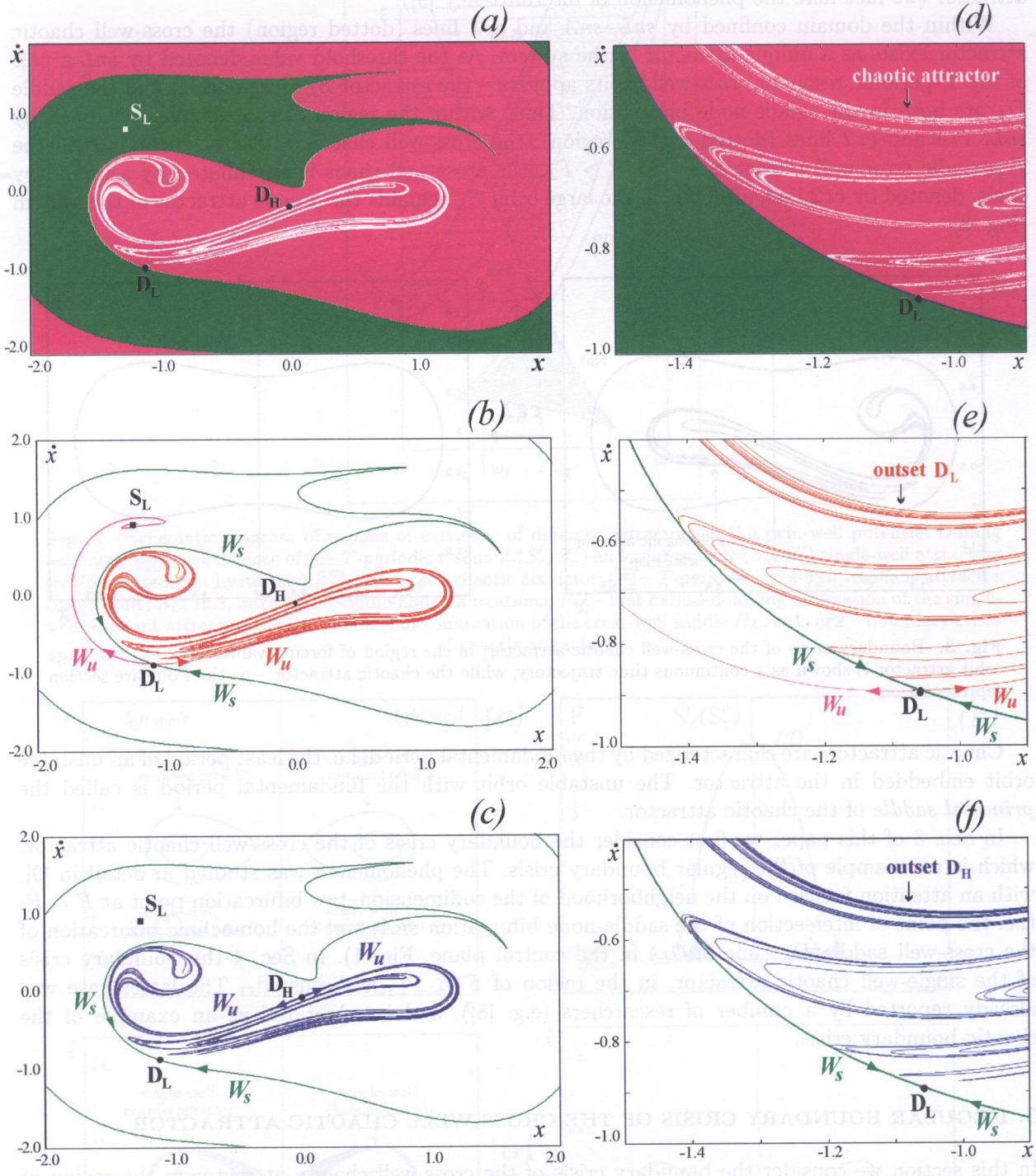

Fig. 4. Basins of attraction and the relevant invariant manifolds (in the $x - \dot{x}$ plane), prior to the regular boundary crisis of the cross-well chaotic attractor; (a) basins of attraction of the two cross-well coexisting attractors: the chaotic attractor (magenta), and the large orbit attractor S_L (green), in a large domain of the phase plane; the Poincaré map of the cross-well chaotic attractor depicted in white; (b) the corresponding family of the invariant manifolds of the destroyer saddle D_L; (c) insets of the destroyer saddle D_L, and outsets of the principal saddle of the chaotic attractor, D_H; (d)–(f) the corresponding blown-up pictures at the boundary crisis bifurcational parameters: (d) "collision" of the chaotic attractor with the destroyer saddle D_L; (e) homoclinic bifurcation of the destroyer saddle D_L; (f) heteroclinic bifurcation of the destroyer saddle D_L, and the principal saddle of the chaotic attractor, D_H

the chaotic attractor tends to the coexisting attractor S_L, and the other outset tends to the chaotic attractor and forms the closure of it. The conclusion is that the boundary crisis of the cross-well chaotic attractor is regular (the destroyer is a regular saddle). Upon further change of the system parameters, as the boundary crisis is approached, the stable manifold (basin boundary) and the unstable manifold (closure of the chaotic attractor) of D_L approach each other, become tangent, and then intersect transversely. The situation for the tangency, i.e. at the homoclinic bifurcation of the saddle D_L, is shown in blown-up pictures in Figs. 4d and 4e. By geometrical evidence, the event can be also interpreted as a "collision" of the chaotic attractor with the destroyer saddle. It follows that the boundary crisis of the cross-well chaotic attractor is catalyzed by the homoclinic bifurcation of the T-periodic saddle D_L (line hbD_L in Fig. 1). In fact, at $F > F_2$, both critical lines shown in Fig. 1, hbD_L and **cr2**, coincide.

In the paper we add some new observations. In Fig. 4c, the insets of the destroyer saddle D_L, and the outsets of the principal saddle of the chaotic attractor, D_H, are shown. We notice that the structure of the right-hand side outset of D_L (depicted in red in Fig. 4b) and that of the outsets of D_H (depicted in blue in Fig. 4c) are extremely close in the phase space. By numerical evidence we realize that the both structures form the closure of the chaotic attractor and, therefore, look exactly like the Poincaré section representation of the attractor (depicted in white in Fig. 4a). The critical crisis parameter values were computed twice: first we determined the tangency condition of the inset and the right-hand side outset of the saddle D_L (Fig. 4e), and then we found the tangency condition of the insets of D_L and the outsets of D_H, which define the heteroclinic bifurcation of the saddles (Fig. 4f). Thus we verified that both types of the global bifurcation: the homoclinic bifurcation of the destroyer saddle, and the heteroclinic bifurcation of the destroyer saddle and the principal saddle of the chaotic attractor, take place at the same values of the bifurcation parameters F, ω, and therefore, they both define the criterion for the boundary crisis to occur.

After the crisis, the cross-well chaotic attractor is erased from the phase space together with its basin of attraction; the large orbit S_L remains the unique attractor in the system, and its basin of attraction invades the whole phase plane (in the considered range of phase parameters). Therefore, the ensuing trajectory of the vanishing chaotic attractor finds itself inside the regular basin of S_L, and the final "jump" of the transient motion is predictable (the outcome is always S_L). Numerical study reveals, however, that the post-crisis transient motion is far from regular behavior. Some of the trajectories, in particular those which initialize from the regions of the phase space where the transverse intersections of the stable and unstable manifolds occur (i.e. which start in the close

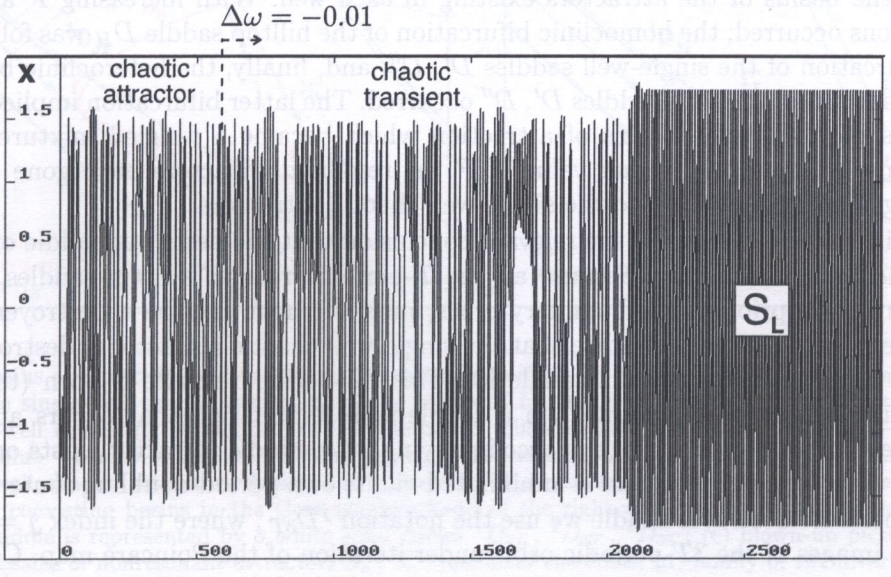

Fig. 5. An example of continuous time-history of the transient response after crisis of the cross-well chaotic attractor, under small step-increment of driving frequency

vicinity of a non-attracting chaotic set), may have long-lasting and chaotic-like time history. An example of such chaotic post-crisis transient response is shown in Fig. 5. It was obtained under small step-increment of driving frequency ω in the close vicinity of the boundary crisis; as a result, the system exhibiting steady-state chaotic oscillations was suddenly set into the region of control parameters where the chaotic attractor ceases to exist. We see that after the crisis the system still realizes the response that looks exactly like the annihilated cross-well chaotic attractor (the trajectory bounces around on its "remnant") for a time that comprises about 250 driving cycles, until the response suddenly settles onto the remote large orbit attractor S_L.

4. Chaotic boundary crisis of the single-well chaotic attractor

In this section we consider the boundary crisis of the single-well chaotic attractor, in the region of forcing amplitude $F < F_1$ (line **cr1**, point **1** in Fig. 1). In this domain, the crisis line **cr1** defines the lower frequency stability limit of the region of primary resonance hysteresis, i.e. the region where the four single-well attractors (two resonant and two nonresonant) coexist. The principal saddle of the single-well chaotic attractor, the attractor which develops from the cascade of period-doublings of the T-periodic resonant attractor $S'_r(S''_r)$, is the T-periodic *inverse saddle* $I'_r(I''_r)$, i.e. the unstable trace of the primary resonant attractor after its first period-doubling bifurcation (Fig. 2b).

To outline the relevant properties of the crisis, first we display the basins of attraction (in the x–$\dot{x}$ plane) of the four coexisting single-well attractors just prior to the boundary crisis (Fig. 6a). The coexisting attractors are two nonresonant T-periodic orbits S'_n, S''_n, and two single-well chaotic attractors (the Poincaré maps of the latter ones are visualized as white bands). Our first observation is that the boundaries of the basins of attraction are not smooth, but form a tangled (fractal) mixture of all four coexisting attractors. In Fig. 6b the blown-up picture of the basins of attraction in a small neighborhood of the right-well chaotic attractor is shown. We clearly see fractal accumulations of the four coexisting basins on the outer side of the small regular area of the chaotic basin.

This fractal structure of the basins of four coexisting attractors was evolved gradually with an increase of the forcing parameter F. Sudden qualitative changes occurred at the threshold values defined by the global bifurcations of the coexisting T-periodic saddles [10]. At low values of F, before any global bifurcation, the basin boundary of the four coexisting attractors were smooth lines: the insets of the single-well saddles D', D'' defined the boundary between the basins of the resonant and nonresonant attractors in the left and right well, respectively, and the insets of the hilltop saddle D_H separated the basins of the attractors existing in each well. With increasing F a sequence of global bifurcations occurred; the homoclinic bifurcation of the hilltop saddle D_H was followed by the homoclinic bifurcation of the single-well saddles D', D'', and, finally, the heteroclinic bifurcation of the saddle D_H and the single-well saddles D', D'' occurred. The latter bifurcation implied a dramatic change in the structure of the basins of attraction which became a tangled mixture of the four coexisting basins. At a slightly higher value of F the resonant attractors undergone a cascade of period doublings and then evolved to the single-well chaotic attractors.

The above situation also leads to the relevant conclusion that the destroyer saddle of the boundary crisis should be subharmonic (because all the T-periodic regular system saddles experienced homoclinic bifurcation prior to the boundary crisis, none of them may be a destroyer saddle). In fact, results of earlier investigations state that the single-well chaotic attractor is destroyed in a collision with the single-well $3T$-periodic saddle [8]. This $3T$-periodic saddle is born (together with the accompanying $3T$-periodic attractor) in a saddle-node bifurcation that occurs at the forcing parameter values far below the crisis (the accompanying $3T$-periodic attractor exists only in a very narrow band of control parameters and is annihilated via its own period-doubling route to crisis [6]).

For the $3T$-periodic destroyer saddle we use the notation ${}^jD_{3T}$, where the index $j = 1, 2, 3$ identifies successive images of the $3T$-periodic orbit under iteration of the Poincaré map. Consequently, in the Poincaré section representation, the invariant manifold of the saddle consists of three parts, each of them evolving from the corresponding image point ${}^1D_{3T}$, ${}^2D_{3T}$, ${}^3D_{3T}$.

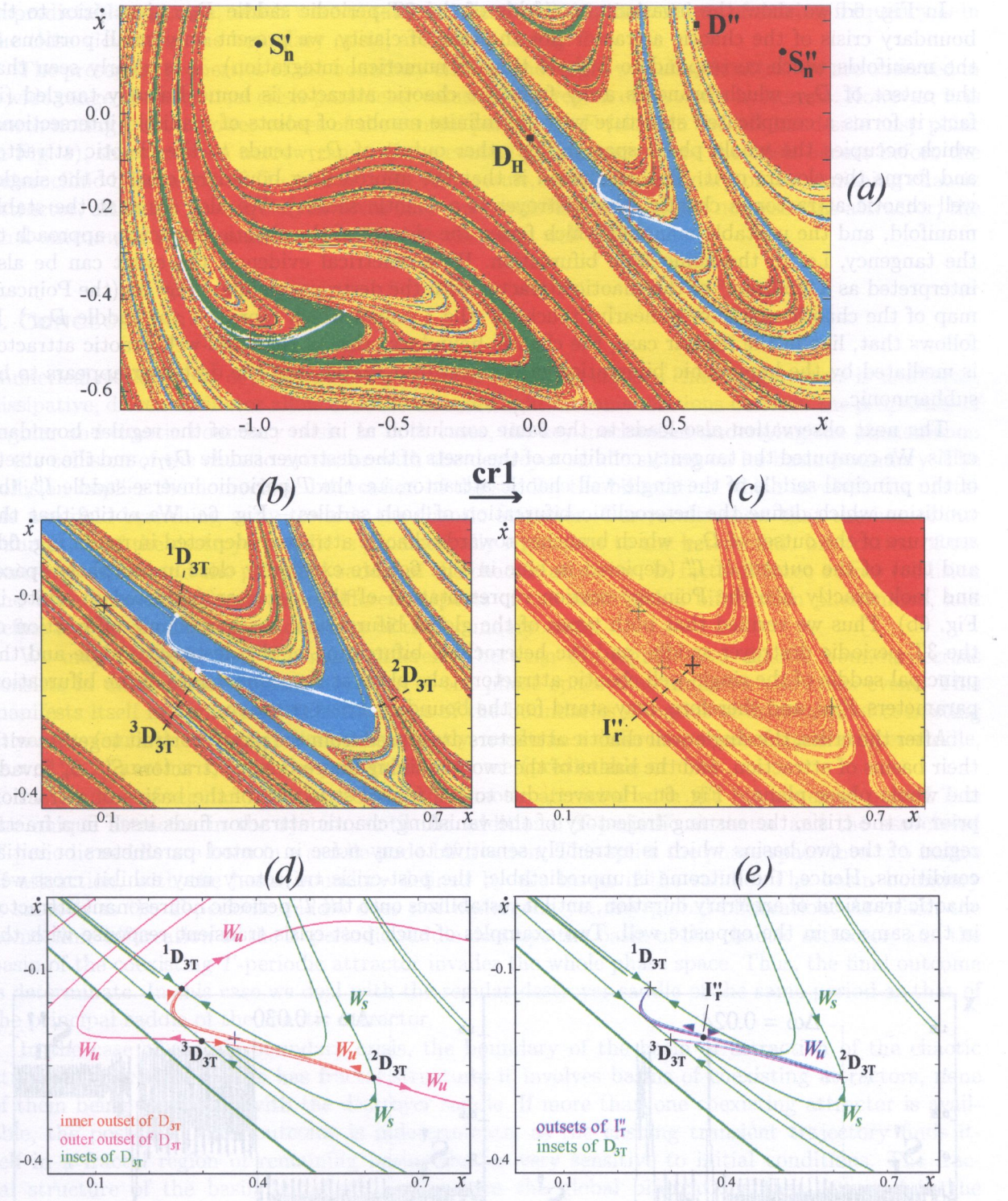

Fig. 6. Basins of attraction and the relevant invariant manifolds (in the x–$\dot{x}$ plane) at the chaotic boundary crisis of the single-well chaotic attractor, in the region of forcing $F < F_1$; (a) basins of attraction of the four single-well coexisting attractors prior to the crisis: yellow depicts the basin of S'_n, red – basin of S''_n, green and blue – basins of the left-well and the right-well chaotic attractor, respectively; Poincaré maps of the single-well chaotic attractors depicted in white (the grid resolution is 960 × 544); (b) blown-up picture of the four coexisting basins in the close neighborhood of the right-well chaotic attractor; the $3T$-periodic destroyer saddle is represented by 3 white solid circles $^1D_{3T}$, $^2D_{3T}$, $^3D_{3T}$; (c) blown-up picture of the two remaining basins of nonresonant attractors S'_n, S''_n, just after the crisis; (d) family of the invariant manifolds of the subharmonic destroyer saddle D_{3T}, just prior to the crisis; (e) the corresponding insets of the destroyer saddle D_{3T}, and outsets of the principal saddle of the right-well chaotic attractor, I''_r

In Fig. 6d we show the invariant manifolds of the $3T$-periodic saddle D_{3T}, just prior to the boundary crisis of the chaotic attractor (for the sake of clarity, we present only small portions of the manifolds which correspond to a short time of numerical integration). It is clearly seen that the outset of D_{3T} which branches away from the chaotic attractor is homoclinically tangled (in fact, it forms a complicated structure with an infinite number of points of manifold intersections, which occupies the whole phase space). The other outset of D_{3T} tends to the chaotic attractor and forms the closure of it. The conclusion is that the approaching boundary crisis of the single-well chaotic attractor is chaotic (the destroyer is a chaotic saddle). We also see that the stable manifold, and the unstable manifold which forms the closure of the chaotic attractor, approach to the tangency, i.e. to the homoclinic bifurcation. By geometrical evidence, the event can be also interpreted as a "collision" of the chaotic attractor with the destroyer saddle – Fig. 6b (the Poincaré map of the chaotic attractor is nearly "touching" the 3 points which represent the saddle D_{3T}). It follows that, like in the regular case, the chaotic boundary crisis of the cross-well chaotic attractor is mediated by the homoclinic bifurcation of the destroyer saddle, but the destroyer appears to be subharmonic.

The next observation also leads to the same conclusion as in the case of the regular boundary crisis. We computed the tangency condition of the insets of the destroyer saddle D_{3T}, and the outsets of the principal saddle of the single-well chaotic attractor, i.e. the T-periodic inverse saddle I_r'', the condition which define the heteroclinic bifurcation of both saddles – Fig. 6e. We notice that the structure of the outset of D_{3T} which branches towards chaotic attractor (depicted in red in Fig. 6d) and that of the outsets of I_r'' (depicted in blue in Fig. 6e) are extremely close in the phase space, and look exactly like the Poincaré section representation of the attractor (depicted in white in Fig. 6b). Thus we verified that both types of the global bifurcation: the homoclinic bifurcation of the $3T$-periodic destroyer saddle, and the heteroclinic bifurcation of the destroyer saddle and the principal saddle of the single-well chaotic attractor, take place at the same values of the bifurcation parameters F, ω, and therefore, may stand for the boundary crisis criterion.

After the crisis, the single-well chaotic attractors are erased from the phase portrait together with their basins of attraction, and the basins of the two remaining nonresonant attractors S_n', S_n'' invade the whole phase plane – Fig. 6c. However, due to the fractal structure of the basins of attraction prior to the crisis, the ensuing trajectory of the vanishing chaotic attractor finds itself in a fractal region of the two basins which is extremely sensitive to any noise in control parameters or initial conditions. Hence, the outcome is unpredictable; the post-crisis trajectory may exhibit cross-well chaotic transient of arbitrary duration, until it restabilizes onto the T-periodic nonresonant attractor in the same or in the opposite well. Two examples of such post-crisis transient response with the

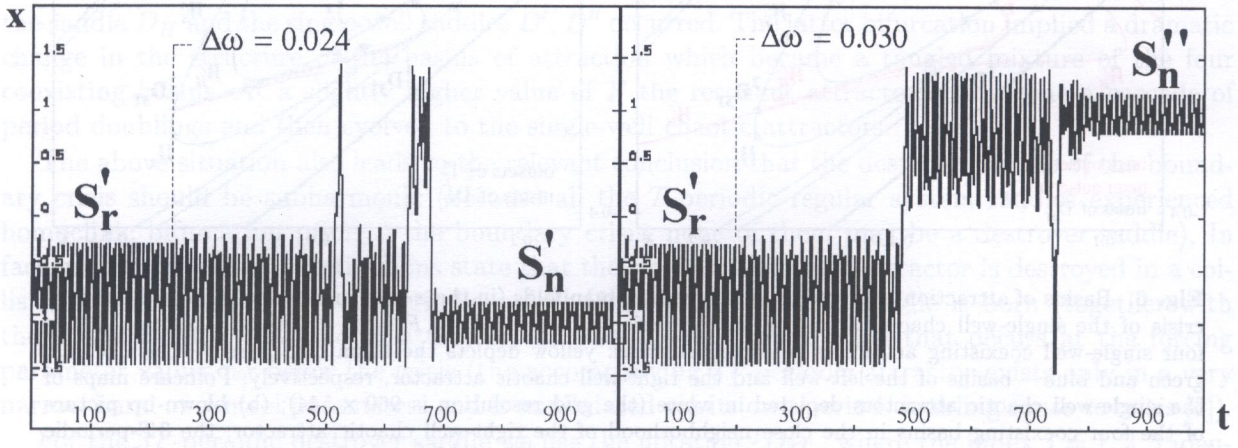

Fig. 7. Two examples of continuous time-history of the transient response with an unpredictable outcome, after annihilation of the single-well resonant attractor S_r' via the boundary crisis scenario; depending on how the bifurcation is realized, the ensuing trajectory, after cross-well chaotic transient, settles onto the nonresonant attractor in the same (S_n') or in the opposite (S_n'') well

unpredictable outcome, which were obtained under small step-increments of driving frequency ω in the close vicinity of the boundary crisis, are shown in Fig. 7.

The presented properties of the boundary crisis of the single-well chaotic attractor are observed in a wide range of the critical crisis parameter values at the region of resonant hysteresis. However, it is worth noting that, at lower values of the control parameter F (close to the left hand-side cusp point in Fig. 1), there exists a narrow range of the control parameters where the crisis occurs before the heteroclinic bifurcation of D_H and D', D''. As a result, the basin boundary of the vanishing chaotic attractor, although not regular, involves only one coexisting basin of the nonresonant attractor; the final outcome is determinate and confined to the same well [10].

5. Conclusions

Numerical explorations of the two examples of the boundary crisis of chaotic attractors in nonlinear, dissipative, driven oscillator allow us to throw more light on some relations between the properties of regular and chaotic boundary crisis. In both cases, the key mechanism underlying the phenomenon is the collision of the chaotic attractor with the destroyer saddle sitting on its basin boundary. The collision implies the homoclinic bifurcation of the saddle, the bifurcation which involves the unstable manifold branching away towards the chaotic attractor. Our results show that the homoclinic bifurcation of the destroyer saddle is geometrically equivalent to the heteroclinic bifurcation of the destroyer saddle and the principal saddle of the chaotic attractor. In fact, all three events (collision and both bifurcations) are three different aspects of the same global bifurcation phenomena, and define the criterion for the occurrence of the boundary crisis.

We may conclude that the main difference between the regular and chaotic boundary crisis consists in different topological structure of the phase space that underlies the crisis event. This manifests itself in apparently different types of the boundaries of basins of attraction of coexisting attractors (smooth or fractal), and, consequently, results in a different period of the destroyer saddle, as well as in another type of the post-crisis outcome (predictable or not).

In the case of regular boundary crisis, the chaotic attractor with the fundamental period T is the unique attractor in the system, until the additional T-periodic attractor and the associated T-periodic saddle are born in a saddle-node bifurcation. This splits the phase space into two basins of attraction, with the basin boundary defined by the insets if the saddle. The basin boundary is smooth as the T-periodic saddle does not undergone yet any global bifurcation. At crisis, the homoclinic bifurcation of the T-periodic saddle destroys the basin of the chaotic attractor, and the basin of the coexisting T-periodic attractor invades the whole phase space. Thus, the final outcome is determinate. In this case we deal with the regular destroyer saddle of the same period as that of the principal saddle of the chaotic attractor.

In the case of chaotic boundary crisis, the boundary of the basin of attraction of the chaotic attractor prior to the crisis has fractal structure; it involves basins of coexisting attractors, none of them being associated with the destroyer saddle. If more than one coexisting attractor is available, the post-crisis final outcome is indeterminate, as the ensuing transient trajectory finds itself in a fractal region of remaining basins that is very sensitive to initial conditions. The fractal structure of the basin boundary results from the global bifurcations that occurred in the system before the generation of a chaotic attractor. In the twin-well potential system and the single-well chaotic attractor with the fundamental period T, the key event is the homoclinic bifurcation of the single-well saddle, which, at low values of the forcing parameter F, defines the smooth, regular basin boundary of the resonant and nonresonant single-well attractors. As a result, when the T-periodic resonant attractor loses its stability and develops into chaotic attractor, there is no T-periodic saddle sitting on its basin boundary. Therefore, the new type of a destroyer saddle is necessary to form a mechanism of erasing the attractor from the phase space, namely the subharmonic one ($3T$-periodic in our example). The subharmonic destroyer saddle appears to be a chaotic saddle (its outset branching away from the chaotic attractor is

homoclinically tangled), and is not associated at crisis with any coexisting subharmonic attractor.

We face the corresponding examples of the regular and chaotic boundary crisis in other systems, as well in other regions of control space [11]. It is worth noting that the phenomenon of boundary crisis, especially the chaotic one, still attracts an interest of applied physicists and mathematicians, and it warrants further study.

APPENDIX

For the sake of clarity, we recall the following fundamental concepts of the nonlinear dynamics of dissipative systems, which we make use of:

Attractor – steady-state stable solution (point, cycle or chaotic orbit);

Saddle – steady-state unstable solution (point, cycle or chaotic orbit), which repels in some phase directions but attracts in others;

Basin of attraction of an attractor – the domain of all initial conditions in the phase plane x–$\dot{x}$, whose trajectories converge to that attractor.

Principal saddle of a chaotic attractor – the least-period unstable solution (a saddle) which is embedded in the chaotic attractor.

Saddle-node bifurcation – the local bifurcation in which the control paths of stable and unstable solution of the same period meet, and both solutions coalesce.

Stable manifold (inset) of a saddle – the invariant set of all initial conditions whose trajectories approach the saddle as $t \to \infty$; it represents the phase attracting direction of a saddle.

Unstable manifold (outset) of a saddle – the invariant set of all initial conditions whose trajectories approach the saddle as $t \to -\infty$; it represents the phase repelling direction of a saddle.

Poincaré section – phase-plane obtained by "stroboscopical sampling" of the phase-space coordinates $(x, \dot{x}, t)$ of the trajectory $x(t)$ in discrete times $t = nT$ $(n = 0, 1, 2 \ldots)$, where $T = 2\pi/\omega$ is the period of driving force. Hence, in the Poincaré section, the T-periodic oscillation is represented by one point, $2T$-periodic – by two points etc.

Homoclinic (heteroclinic) bifurcation – tangency of stable and unstable manifolds of the saddle (or two different coexisting saddles, respectively) in the phase-space, which, at further sweep of the control parameter, implies an infinite number of transversal intersections of the manifolds, giving rise to a highly complicated, chaotic dynamics.

Fractal structure – highly intertwined, fine-scale structure with a fractional (non-integer) dimension greater than one, which involves basins of attraction of multiple coexisting attractors. It results from the global bifurcations of the basins (homoclinic/heteroclinic) and gives rise to sensitive dependence on initial conditions, long-lasting chaotic transients, and an unpredictability of the final outcome.

REFERENCES

[1] M.J. Feigenbaum. Quantitative universality for a class of nonlinear transformations. *J. Stat. Phys.*, **19**: 25–52, 1978.

[2] C. Grebogi, E. Ott, J.A. Yorke. Crises, sudden changes in chaotic attractors and transient chaos. *Physica*, **D7**: 181–200, 1983.

[3] A.L. Katz, E.H. Dowell. From single-well chaos to cross-well chaos: a detailed explanation in terms of manifold intersections. *Int. J. Bifurcation and Chaos*, **4**(4): 933–941, 1994.
[4] H.E. Nusse, J.A. Yorke. *Dynamics: Numerical Explorations*. Springer-Verlag, New York, 1998.
[5] E. Ott. *Chaos in Dynamical Systems*. Cambridge University Press, Cambridge, 1993.
[6] M.S. Soliman, J.M.T. Thompson. Basin organization prior to a tangled saddle-node bifurcation. *Int. J. Bifurcation and Chaos*, **1**(1): 107–118, 1991.
[7] J.C. Sommerer, C. Grebogi. Determination of crisis parameter values by direct observation of manifold tangencies. *Int. J. Bifurcation and Chaos*, **2**(2): 383–396, 1992.
[8] H.B. Stewart, Y. Ueda. Catastrophes with indeterminate outcome. *Proc. Roy. Soc. Lond.*, **A432**: 113–123, 1991.
[9] W. Szemplińska-Stupnicka, K.L. Janicki. Basin boundary bifurcations and boundary crisis in the twin-well Duffing oscillator: scenarios related to the saddle of the large resonant orbit. *Int. J. Bifurcation and Chaos*, **7**(1): 129–146, 1997.
[10] W. Szemplińska-Stupnicka, E. Tyrkiel. Sequences of global bifurcations and the related outcomes after crisis of the resonant attractor in a nonlinear oscillator. *Int. J. Bifurcation and Chaos*, **7**(11): 2437–2457, 1997.
[11] W. Szemplińska-Stupnicka, A. Zubrzycki, E. Tyrkiel. Properties of chaotic and regular boundary crisis in dissipative driven nonlinear oscillators. *Nonlinear Dynamics*, **19**: 19–36, 1999.
[12] W. Szemplińska-Stupnicka, E. Tyrkiel, A. Zubrzycki. Chaotic oscillations in a model of suspended elastic cable under planar excitation. *Computer Assisted Mech. Engng. Sci.*, **6**: 217–229, 1999.
[13] J.M.T. Thompson, H.B. Stewart, Y. Ueda. Safe, explosive and dangerous bifurcations in dissipative dynamical systems. *Phys. Rev.* **E 49**(2): 1019–1027, 1994.
[14] Y. Ueda, S. Yoshida, H.B. Stewart, J.M.T. Thompson. Basin explosions and escape phenomena in the twin-well Duffing oscillator: Compound global bifurcations organizing behavior. *Phil. Trans. Roy. Soc. London* **A332**: 169–186, 1990.